International Journal of Production Research, 2017
https://doi.org/10.1080/00207543.2017.1356484

Robust design optimization via surrogate network model and soft outer array design

Jyh-Cheng Yu[a1], Chaio-Kai Chang[a], and Suprayitno[a,b]

[a]*Department of Mechanical and Automation Engineering, National Kaohsiung First University of Science and Technology, Kaohsiung 811, Taiwan, ROC.;* [b]*Department of Mechanical Engineering, State University of Malang, Indonesia*

(Received 27 November 2016; accepted 12 July 2017; Published online: 28 Jul 2017)

Robust design searches for a performance optimum with least sensitivity to variable and parameter variations. Taguchi method applies an inner array for control factors and an outer array for noise factors to estimate the Signal-to-Noise ratio (S/N). However, the cross product arrays impose serious cost concerns for expensive samplings. Also, rigorous control of noise factors to pre-set levels is impractical in industrial applications. This study presents a soft computing-based robust optimization that merges control and noise factors into a combined experimental design to establish a surrogate using artificial neural network. Genetic algorithm is applied to search in the sub-space of control factors in the surrogate with a soft outer array to estimate the S/N served as the evolution fitness. Performance variations due to the tolerances of control and uncontrollable factors can then be estimated without conducting actual experiments. The verifications of the predicted optima become additional learning samples to refine the surrogate, and the iteration continues until convergence. The robust optimization of a micro-accelerometer with maximized gain is used as an illustrative example. The proposed algorithm provides a superior robust optimum using a much smaller sample and less controlling cost compared with Taguchi method and a conventional response surface method.

Keywords: Robust Design, Robust Optimization, Taguchi Methods, Neural Network applications, Genetic Algorithms, Expensive Optimization, Accelerometer

1. Introduction

Engineering designs are subject to the variations of manufacturing, operational conditions, and property deterioration. Quality engineering aims to ensure the performance to specification despite these variations. Tolerance control reduces performance deviation by tightening the tolerances of design parameters, which often results in cost increase. Robust design such as Taguchi method (Taguchi, 1978) considers the influence of life-cycle uncertainties and applies parameter design to search for the optimum with quality performance. Taguchi method is adapted from fractional factorial experiments featuring signal-to-noise ratio (S/N), orthogonal arrays (OA), and analysis of means (ANOM). The optimal combination of parameter levels with maximum S/N is identified from the effect analysis to improve the average performance and at the mean time to reduce the performance deviation. Many successful applications had been reported in the literature (Gamage et al. 2014, Irad 2005, Sun et al. 2015, Lin and Yang 2017). Ouyang et al. (2016) argued that parameter uncertainties in noise factors are typically neglected in determining robust input settings, and proposed an interval approach to account the parameter uncertainties derived from noise variables and response models. Mondal et al. (2014) compared the robustness modelling and the robustness indices including their strength, limitation, and applicability under different process conditions.

For the design problems with analytical models, the propagation of variance method can be applied to reformulate the analytic model to integrate the parameter uncertainties (Picheral *et al.* 2014). However in most engineering applications without analytical models, the statistical indices of the response of a design treatment such as the mean and variance due to the influence of noise factors have to be estimated using sampling. The sampling strategy using experimental design of the noise factors will provide better and efficient estimations than random sampling. The Taguchi experimental design adopts a cross array design consisting of an inner orthogonal array for the control factors and an outer array for the noise factors to estimate the S/N of a design treatment due to the life-cycle uncertainties. Noise factors such as manufacturing errors, variations of parameter, deterioration, and uncertainties of operational conditions are arranged in a fractional factorial array to ensure a symmetric distribution of a small sample. The use of outer array to estimate the distribution of design performance in product life cycle is theoretically sound; however, the control of noise factors to a specific preset level in the outer array is expensive and impractical in engineering applications.

Despite the popularity in industrial applications, some also commented on the limitations and inefficiencies of the Taguchi method (Maghsoodloo *et al*., 2004). Reducing the number of experiments and sampling costs is very

[1] Corresponding author: Jyh-Cheng Yu, jcyu@nkfust.edu.tw

important in robust engineering optimization. The total number of the Taguchi experimental design is the product of the sizes of inner and outer arrays, which multiplies rapidly as the number of factors increasing. For instance of four three-level control factors and six two-level noise factors, an L18 inner array and an L8 outer array will require at least 144 experiments in total. The number of experiments and the high controlling cost in outer array become a liability for the robust design of engineering application using Taguchi method. Also, Taguchi's parameter design assumes a linear model and uses the analysis of means (ANOM) to find the optimal factorial combination that is sensitive to interaction effects, and the optimum is constrained to the preset level of control factors. Any missing data and deviation from the level control in the experimental design will result in analytical difficulties.

Surrogate-based optimization is an effective alternative that replaces the engineering system with an approximate surrogate model trained from the sampled data to predict the system response (Bhattacharya 2013, Forrester and Keane 2009, Tenne 2012). Typical surrogate techniques include Polynomial Response Surface Method (RSM) (Bota *et al.* 2000 and Moyo *et al.* 2003), Kriging (Bhattacharya 2013), and Artificial Neural Network (Zeidenberg 1990). The optimum can then be predicted by applying an optimizer to the surrogate model without direct interaction with the engineering system. However, the generality of the surrogate is directly related to the number and distribution of samples. Since large initial samples are not economically feasible to industrial applications, many literatures suggested progressive modeling and iterative search (Jin *et al.* 2002, Yu and Juang 2010). Design of experiments is first applied to establish the initial surrogate followed by sequential infilling sampling (Forrester and Keane 2009, Parr *et al*. 2012) to distribute new sample(s) at promising areas in an iterative fashion to improve the regional accuracy of the progressive surrogate.

The applications of the surrogate-based optimization to robust design have to provide the estimation of response distribution due to noise factors. Some (Yeniay *et al*. 2006, Hou and Zhang 2017) combined Taguchi's experimental design and response surface methods to predict the robustness index such as mean, standard deviation, and S/N. A quadratic polynomial RSM model is often adopted in applications as a surrogate and an optimizer is applied to search for the robust optimum. Some suggested more realistic and complex models such as Kriging, Radial Basis Function (RBF), and Radial Basis Function Neural Network (RBFNN) to estimate the mean and variance of the highly nonlinear input/output response (Elsayed and Lacor 2014). Dual response surface methods (Vining and Myers 1990) constructed one model for the mean and another for the variance of the system response from crossed OA experiments. In contrast, single response surface methods establish a surrogate model to estimate the robustness metrics such as S/N directly (Dellino *et al.* 2012). However, the direct use of the cross array design for the estimation of the robustness index will impose a high sampling cost on engineering applications. Köksoy (2008) suggested a combined array consisted of control and noise variables to model the response using a quadratic approximation, and estimated the response variances using the propagation-of-error modeling. A robust optimum can then be derived by minimizing the mean square error (MSE) criterion based on Taguchi's average quality loss (Lin and Tu 1995). However, the selection of polynomials is challenging for a complex engineering system. Also, a second-order response surface model may not be sufficient, but high order polynomials will significantly increase the minimal number of experiments required as the number of factors increase.

Artificial neural networks (ANNs) are a family of statistical learning models inspired by biological neural networks consisted of interconnected "neurons" which send messages to each other. The numeric weights of connections can be tuned using the learning samples to establish a surrogate model to predict system response. ANN is often applied to establish a surrogate model of complex systems (Chen *et al.* 1998, Sarve *et al.* 2015). To ensure the quality of sample distribution, orthogonal arrays are often introduced to the design of training experiments (Benardos and Vosniakos 2002, Su *et al.* 2012). However, the feature of Taguchi's robust design scheme considers the influence of noise factors on performance distribution and uses outer array to estimate the S/N of a parameter design. Wang *et al*. (1998) applied the cross array experiments to set up a multilayer feedforward neural network to predict mean and variance of the response for a parameter design. A robust design analysis is then constructed on the basis of the neural network. However, the ANN surrogate model considers only control factors. High sample number and controlling cost due to the use of outer array are still unaddressed issues. Some surrogate-based optimization proposed to include both control and noise factors into a single planned experiments by a combined array approach to reduce the number of experiments, and apply the propagation of error modeling to estimate the variances (Köksoy 2008).

This paper proposes a soft computing-based robust optimization methodology for engineering applications with expensive experimental samples. A surrogate model using artificial neural network is first established from a combined experimental design with both design variables and parameters. A soft outer array is introduced to estimate the robustness measure that served as the design fitness for the evolutionary search in the subspace of control factors. The robust design of a piezoelectric micro-accelerometer with maximized measurement gain is used as a case study to illustrate the merits of the proposed optimization scheme.

2. Robust optimization using surrogate network model

The Taguchi experimental design applies a cross array design consisted of an inner array for control factors and an outer array for noise factors. The number of the cross array design will multiply dramatically. Also, rigorous control

of noise factors to specific pre-set levels in outer array will be impractical and expensive in engineering applications. To cope with the constraints of Taguchi method, this study proposes a soft computing-based robust optimization methodology. Both control and noise factors are merged into a combined experimental design that serves as learning samples to set up a surrogate model using artificial neural network. Evolutionary optimizer is applied to search in the subspace of control factors of the ANN surrogate for the robust optimum. A soft outer array is introduced to the parameter design to estimate the S/N using the surrogate that served as the fitness in the evolutionary optimization. The searched optimum is verified using the engineering system and introduced to the learning samples to retrain the surrogate. The process iterates until the convergence of the robust optimum. The complete flow chart of the proposed scheme, surrogate-based robust optimization (SURO), is shown in Fig. 1 which will be elaborated in the following sections.

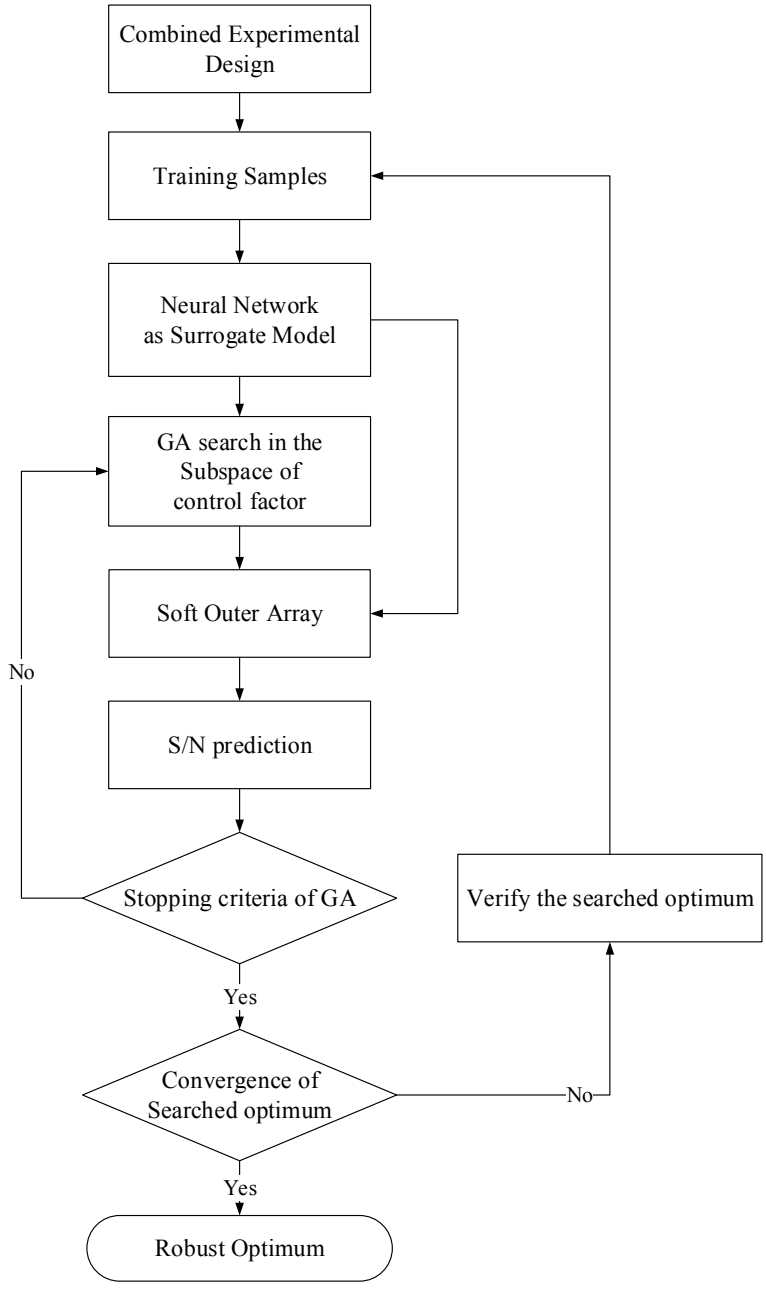

Fig. 1 Flow chart of Surrogate Robust Optimization (SURO)

2.1. Neural network surrogate from a combined experimental design

This study applies a combined experimental design as the training samples for a surrogate model using ANN. The noise factors due to manufacturing tolerances and deterioration of control factors can be estimated from the surrogate model, and thus can be neglected in the experimental design to reduce the number of experiments. For the example

of four three-level control factors: *A, B, C*, *D* and six two-level noise factors, the noise factors include four manufacturing tolerances of control factors: N_A, N_B, N_C and N_D, an outer noise factor T, and the variation of a system parameter P. A typical Taguchi experimental design requires an L18 inner array and an L8 outer array, which will account for at least 144 experiments in total. The combined experimental design will consider only six independent factors: *A, B, C*, *D, T,* and *P*, which can be deployed in a smaller fractional factorial of three-level such as L18 orthogonal array.

The training samples of ANN often include learning samples and validation samples (Zeidenberg 1990). The error of the validation samples are used as the criteria of early stop to prevent overfitting of network. All the control factors are selected as three-Level in this study for the experimental design of leaning samples. The validation samples suggests a two-level design that is selected in between the levels of the learning samples. For the previous learning samples of six factors, the smallest validation samples could be a L8 orthogonal array. Larger orthogonal arrays can be adopted with better prediction accuracy for the trained surrogate at the expense of a higher sample cost. The experimental designs ensure even distribution of training samples. However, the level settings are used as a reference and exact control to the designated levels are not required. Since the parameter values and the corresponding response of each sample will serve as the training samples of ANN, the exact values even different from the preset level can still be used to train the network surrogate.

2.2. Estimation of design robustness using soft outer array

The surrogate model can estimate the system response for a given instance of control and noise factors. Since the parameter design considers only the control factors, an evolutionary optimizer such as genetic algorithm is then applied to search the subspace of control variables for the robust optimum. The design performance of every individuals in the population will have a stochastic distribution due to the presence of noise factors. This study proposes a 'soft outer array' to estimate the S/N of a parameter design using the surrogate model that served as the fitness for the evolutionary search of the robust optimum. The performance perturbations due to the noise factors are estimated from the surrogate model rather than actual experiments. Depending on the performance requirement, three types of S/N adapted from Taguchi's philosophy of average quality loss are defined as follows:

1. Smaller-the-better: The designer is interested in minimizing the response. The fitness function is given by

$$S/N_{\mathrm{STB}} = -10 \cdot \log_{10}\left(\frac{1}{n}\sum_{i=1}^{n} y_i^2\right) \tag{1}$$

2. Larger-the-better: The designer is interested in maximizing the response. The fitness function is given by

$$S/N_{\mathrm{LTB}} = -10 \cdot \log_{10}\left(\frac{1}{n}\sum_{i=1}^{n} \frac{1}{y_i^2}\right) \tag{2}$$

3. Nominal-the-best: The designer wishes for the response to attain a certain target value. The fitness function is given by

$$S/N_{\mathrm{NTB}} = -10 \cdot \log_{10}\left(\frac{1}{n}\sum_{i=1}^{n} (y_i - m)^2\right) \tag{3}$$

where y_i are the predicted responses from the soft outer array sampling, n is the number of samples in the outer array, and m is the design target value.

Since the response variations in the outer array samples are estimated using the recall of surrogate model rather than actual experiments, the number of samples of the soft outer array will not incur additional sample cost. The proposed scheme can reduces the number of experiments and the control costs of outer array sampling in the evaluation of robustness measure.

2.3. Iterative robust design optimization

This study applies GA to be the evolutionary optimizer for robust parameter design. The training samples of the ANN surrogate are used to be the initial population of GA search. The surrogate accuracy will depend on the number of training samples that will be in proportional to the sampling cost. For expensive optimization, the number of samples will be a constraint. This study suggests a smaller initial sample, and improves the surrogate in an iterative fashion. Since the generality of the initial surrogate may be inadequate depending on the model complexity and the number of training samples, the optimal parameter design provided by the GA search is only a predicted optimum. The verification result of the predicted optimum using actual experiment can be used to evaluate the generality of surrogate, and serves as an additional learning sample to retrain and refine the surrogate model. The training and search process iterates until the convergence of the robust optimum.

3. Robust Design of Micro-accelerometer

3.1. Design and simulation of Piezoelectric Micro-accelerometer

Robust design of a piezoelectric micro-accelerometer which involves in complicated sequential fabrication procedures serves as an illustrative example for the application of proposed scheme SURO. The design objective is to increase the measurement gain and quality. The sample piezoelectric micro-accelerometer in this study consists of four symmetric beam suspensions with eight piezoelectric transducers and a seismic mass as shown in Yu and Lan (2001). Two piezoelectric thin film transducers are patterned on each suspension beam. One is near the fixed end and the other is near the seismic mass. The piezoelectric transducer is composed of an upper electrode, a piezoelectric thin film, and a lower electrode.

This study considers only the first vibration mode because the resonant frequency of the second vibration mode is about twice that of the first vibration mode. The supporting beams deflect symmetrically as shown in Fig. 2(a) for the first vibration mode. All the outer transducers are of the same bending direction which is opposite to the inner transducers. On the other hand, in the second vibration mode as shown in Fig. 2(b), two beams are subject to asymmetric bending and the other two beams are subject to torsion. The generated charge due to torsion is negligible compared with that due to bending. The proposed design suggests that the upper electrodes of the outer transducers are connected with the lower electrodes of the inner transducers, and the lower electrodes of the outer transducers are connected with the upper electrodes of the inner transducers, as shown in Fig. 3(a). The interconnected design will double up the transducer gain for the first vibration mode while cancel out the charge due to the second vibration mode and unexpected noises to increase the measurement selectivity (Yu and Lan 2001).

The device can be fabricated from the wet etching of {100} SOI silicon (Seidel *et al.* 1990) and dry etching of suspension beams (Sze 1994). The structure variables considered here include the length of beam suspension l_b, the width of beam suspension w_b, the thickness of beam suspension t_b, the length of the seismic mass l_m and the thickness of the seismic mass h_m. Typical frequency bandwidth, using ±5% as an accuracy requirement, is bound between $3/\tau$ and $\omega_n/5$ where τ is the time constant of piezoelectric transducer and ω_n is the mechanical resonance frequency of the sensor structure. Both high gain and wide frequency bandwidth are desired. However, lower resonance frequency increases sensor gain but reduces frequency bandwidth. A trade-off has to be considered between wide frequency bandwidth and high gain.

The design problem consists of five control factors and eleven noise factors. The noise factors include the manufacturing tolerances of microstructure, the uncertainties of material properties, and the variation of signal frequency. The fabrication of the device is very expensive and it is difficult to control the noise factors at the specified level in outer array experiments. This study applies the numerical simulations using ANSYS for sensor gain to illustrate the applications of robust design.

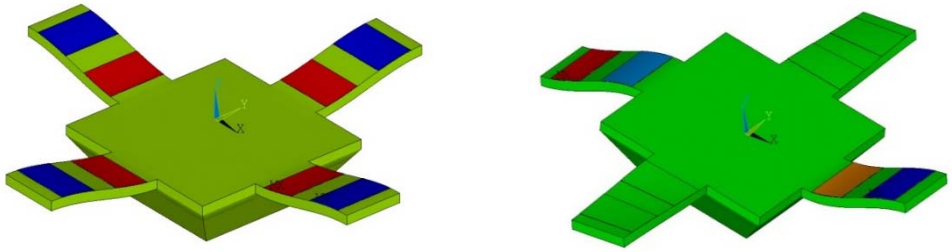

(a) **(b)**

Fig. 2 Schematic vibration of the sample accelerometer (a) first (symmetric) vibration mode (b) second (asymmetric) vibration mode

The initial dimensional design of the sample device is as follows: l_b=400, w_b=200, t_b=30, l_m=600, and h_m=200 (μm) respectively. The ends of the supporting beams are assumed rigid. The FEM model uses only one quarter of the structure and pertinent boundary conditions because of design symmetry to reduce the simulated time. A convergence analysis of the number of mesh is conducted first to make sure the size of mesh is fine enough to estimate correct gain. Typical material properties of sol-gel PZT (Van Kampen and Wolffenbuttel 1998, Xu *et al.* 2000, Yang *et al.* 2014) are used in this study: PZT Young's Modulus E_{PZT} = 79.36 GPa, PZT Permittivity ε = 6.4605×10^{-9} F/m, and PZT Piezoelectric coefficient d_{31} = -93.5×10^{-12} C/N. All the piezoelectric thin films are poled in the same direction along the thickness. Two transducers are patterned symmetrically on each beam. The transducers on the same beam are always of opposite phases as shown in the simulation result.

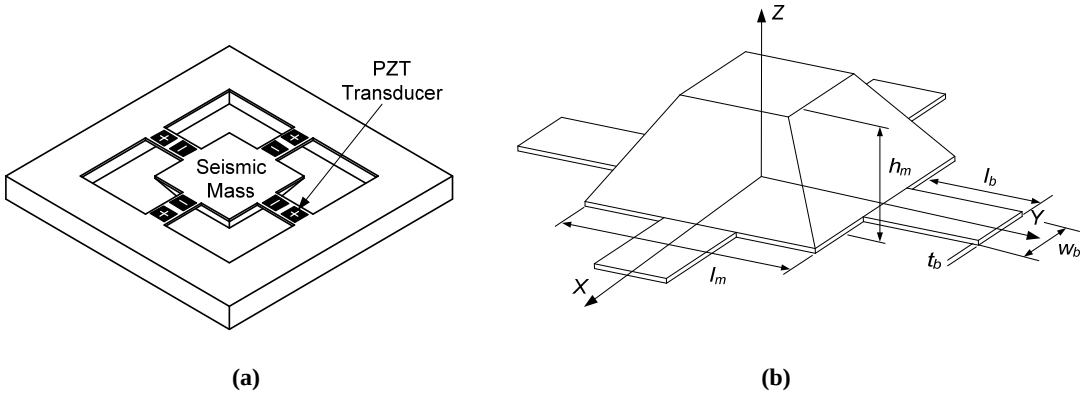

(a) **(b)**

Fig. 3 Schematic deployment of piezoelectric transducers and the dimensional variables of the accelerometer (a) Front View (b) Back View.

3.2. Robust design of Micro-accelerometer using Taguchi Method

Despite its importance, robust optimization is often overlooked in designing accelerometers for mass production because of expensive experimental costs. Design optimization of the accelerometer attempts to maximize the sensor gain under the frequency bandwidth requirement. Performance robustness is crucial in the parameter design of accelerometers to ensure production quality. The output charge of an ideal accelerometer assumes a linear relationship with acting acceleration over the bandwidth as shown in (1). The accelerometer gain is determined mainly by the dimensions of beam suspension, seismic mass, transverse piezoelectric charge to stress ratio, and the electric subsystem. The increasing of the sensor gain will be at the expense of a lower resonant frequency that will reduce the application bandwidth. For a given bandwidth requirement, we would like to search for the dimensional design of an accelerometer with a high gain and linearity despite possible manufacturing errors. The optimization problem can be treated as a larger-the-better problem using Taguchi method. The design objective is to maximize sensor gain β and to reduce the gain deviation due to manufacturing, uncertainties of parameters, deterioration, and variations of operation condition.

$$e = \beta \cdot \ddot{z}_i \tag{4}$$

where β is the sensor gain, e is the output voltage, and $\ddot{z}_i$ is the input acceleration.

A 3-level factorial design is chosen herein for the five control factors. The parameter values of the initial design value are assumed to be the second levels to explore the design space centered at the initial design. Herein a minimal orthogonal array of L18 is selected for the control factors. The gain of each treatment of the control factors varies when the design is in production. The causes of variability come from manufacturing errors, variations of parameter, deterioration, and uncertainties of operational conditions. The initial noise factors considered in this study include the dimensional errors of the microstructure, the fluctuations of the Young's modulus of silicon and PZT thin film ΔE_{Si} and ΔE_{PZT}, the dielectric constant $\Delta\varepsilon$, the piezoelectric constant Δd_{31} of PZT film, and the operating frequency ω of the acceleration as shown in Table 1. There are eleven noise factors where the operating frequency ω in required bandwidth is treated as four-level because of a wide range with nonlinearity, and the rest of noise factors are taken as two-level. A modified L16 orthogonal array with one 4-level column and twelve 2-level columns is selected for the noise factors to determine the significance. The noise factors are applied to the initial design of accelerometer to estimate the corresponding response of each treatment using the ANSYS simulation. The noise effects plot is shown in Fig. 4. The analysis of variance (ANOVA) of the 11 noise factors indicates that the sum of squares (SS) for the operating frequency ω and the manufacturing tolerances of w_b, and h_m are very low. The sum of squares of these three noise factors are then pooled into the error term. ANOVA for the reduced model of 8 noise factors in Table 2 shows that all the noise factors are significant at the level of 5%. Therefore, the L16 outer array is still selected for the eight two-level factors in Taguchi's experimental design to estimate the robustness measure.

The larger-the-better type of average quality loss is adopted to be the robustness measure as shown in (5), where β is the sensor gain, and n is the number of experiments of the outer array for a parameter design.

$$S/N = -10 \cdot \log_{10}\left(\frac{1}{n}\sum_{i=1}^{n}\frac{1}{\beta_i^2}\right) \tag{5}$$

The sensor gains for the crossed experimental design of L18×L16 are simulated using ANSYS to estimate the S/N as shown in Table 3. The effect plot of the control factors using ANOM is shown in Fig. 5. ANOVA of the control factors in Table 4 shows the significance of all the control factors, and the robust optimum can be derived by the parameter design with the maximum S/N as follows: $l_b3 = 500$, $w_b1 = 150$, $t_b2 = 30$, $l_m3 = 800$, and $h_m3 = 300$ (μm). The S/N of the robust design using L16 outer array design and ANSYS analysis is 26.87 dB with a mean gain of

24.02 and a standard deviation of 5.55 (10^{-2} mV/G). The total number of experiments required using Taguchi method is 304 including 288 samples for the crossed array experimental design and the verification runs using L16 for the robust optimum.

Table 1 Level settings for the initial selection of noise factors

	Level 1	Level 2	Level 3	Level 4
ω (Hz)	60	1700	3350	5000
$\Delta\, l_b$ (μm)	-2.0	2.0		
$\Delta\, w_b$ (μm)	-2.0	2.0		
$\Delta\, t_b$ (μm)	-2.0	2.0		
$\Delta\, l_m$ (μm)	-2.0	2.0		
$\Delta\, h_m$ (μm)	-2.0	2.0		
$\Delta\, t_p$ (μm)	-0.1	0.1		
ΔE_{PZT} (%)	-10	10		
ΔE_{Si} (GPa)	-2.0	2.0		
$\Delta\varepsilon$ (%)	-10	10		
Δd_{31} (10^{-12} C/N)	-10	10		

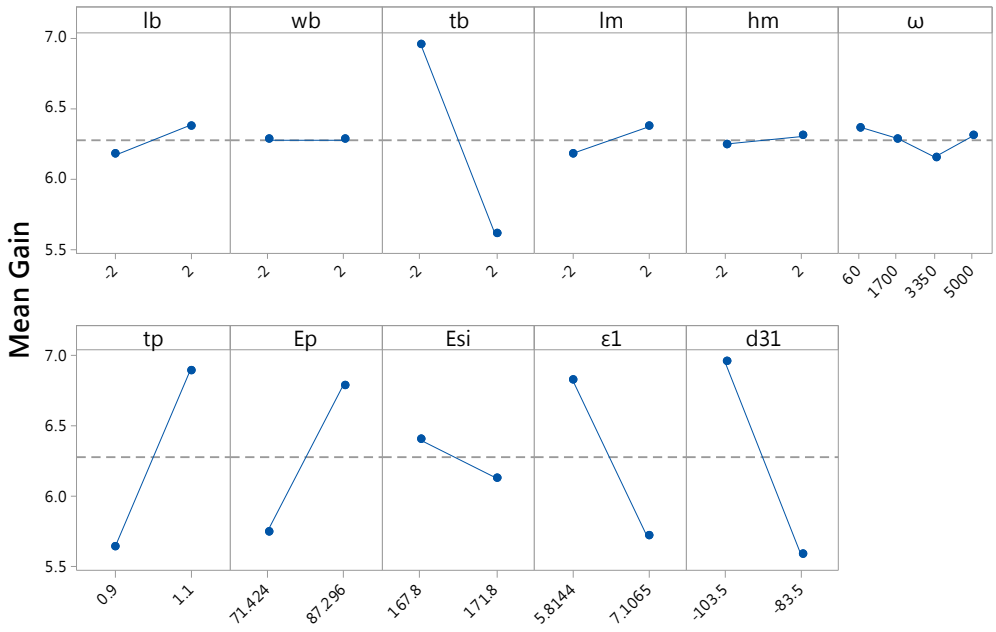

Fig. 4 Effect plot for the initial selection of noise factors

3.3. Robust design of Micro-accelerometer using RSM

The RSM approach using a quadratic model is applied to compare with the result of the proposed scheme. A face-centered central composite design (FCCD) of 27 points with one run of center point is used so the five 3-level control factors can be applied as in Taguchi method. The outer array of L16 is used for the eight significant noise factors as in Taguchi method to estimate the S/N of each design treatment. The experimental design of FCCD27×L16 as shown in Table 5 is used to establish a quadratic response surface model as in (6) for the prediction of S/N.

$$\hat{y}_{S/N} = 2.81 + \mathbf{x}^T\mathbf{b} + \frac{1}{2}\mathbf{x}^T\mathbf{H}\mathbf{x} \tag{6}$$

$$\mathbf{b} = \begin{bmatrix} 0.0438 \\ -0.0910 \\ -1.1487 \\ 0.0626 \\ 0.0606 \end{bmatrix} \quad \mathbf{H} = \begin{bmatrix} -0.0000500 & 0.0000155 & 0.0001025 & -0.0000072 & -0.0000075 \\ 0.0000155 & 0.0002520 & 0.0002250 & -0.0000149 & -0.0000160 \\ 0.0001025 & 0.0002250 & 0.0211654 & -0.0001150 & -0.0001225 \\ -0.0000072 & -0.0000149 & -0.0001150 & -0.0000460 & 0.0000246 \\ -0.0000075 & -0.0000160 & -0.0001225 & 0.0000246 & -0.0001940 \end{bmatrix}$$

where $\mathbf{x}^T$ is the vector of control factors [l_b, w_b, t_b, l_m, h_m].

The predicted optimum in the design space obtained using quadratic programming is l_b = 500, w_b =150, t_b =25, l_m = 800, and h_m = 300 (μm) with a predicted S/N of 29.81 dB. The verified S/N for the robust design from RSM is 29.85 dB. The total number of experiments required using RSM is 448 including 432 samples for the crossed array experimental design and the verification runs using L16 for the robust optimum.

Table 2 ANOVA for the reduced model of noise factors

Source	DF	Adj. SS	Adj. MS	F-Value	P-Value
Δl_b	1	0.172	0.17198	6.5	0.038
Δt_b	1	7.2492	7.24923	273.92	0.00
Δl_m	1	0.1477	0.14772	5.58	0.05
Δt_p	1	6.1703	6.1703	233.15	0.00
ΔE_{PZT}	1	4.3499	4.34992	164.37	0.00
ΔE_{Si}	1	0.3009	0.30091	11.37	0.012
$\Delta\varepsilon$	1	4.9218	4.92181	185.98	0.00
Δd_{31}	1	7.4935	7.4935	283.15	0.00
Error	7	0.1853	0.02646		
Total	15	30.9906			

Table 3 FEM simulation result of the Taguchi cross array experimental design (L18×L16) of piezoelectric micro-accelerometers

L_{18}	l_b (μm)	w_b (μm)	t_b (μm)	l_m (μm)	h_m (μm)	Average Gain* $\beta_{average}$ (10^{-2} mV/G)	Standard Deviation* (10^{-2} mV/G)	S/N** (dB)
1	300	150	25	400	100	2.56	0.55	7.61
2	300	200	30	600	200	4.59	0.97	12.69
3	300	250	35	800	300	6.46	1.36	15.66
4	400	150	25	600	200	11.27	2.40	20.49
5	400	200	30	800	300	14.27	3.00	22.54
6	400	250	35	400	100	1.38	0.29	2.23
7	500	150	30	400	300	5.32	1.12	13.98
8	500	200	35	600	100	4.47	0.94	12.46
9	500	250	25	800	200	16.52	3.51	23.81
10	300	150	35	800	200	8.75	1.84	18.30
11	300	200	25	400	300	3.21	0.69	9.58
12	300	250	30	600	100	2.68	0.57	8.00
13	400	150	30	800	100	10.51	2.21	19.89
14	400	200	35	400	200	2.06	0.43	5.72
15	400	250	25	600	300	8.29	1.76	17.81
16	500	150	35	800	300	18.00	3.77	24.57
17	500	200	25	400	100	3.62	0.77	10.62
18	500	250	30	600	200	6.45	1.36	15.65

* Average and standard deviation of sensitivities are estimated using L16 of significant noise factors

** Larger-the-better S/N using equation (5)

Table 4 ANOVA for the control factors

Source	DF	Adj. SS	Adj. MS	F-Value	P-Value
l_b	2	71.791	35.896	281.41	0.00
w_b	2	41.014	20.507	160.77	0.00
t_b	2	63.392	31.696	248.49	0.00
l_m	2	355.369	177.685	1393.01	0.00
h_m	2	49.486	24.743	193.98	0.00
Error	7	0.893	0.128		
Total	17	709.945			

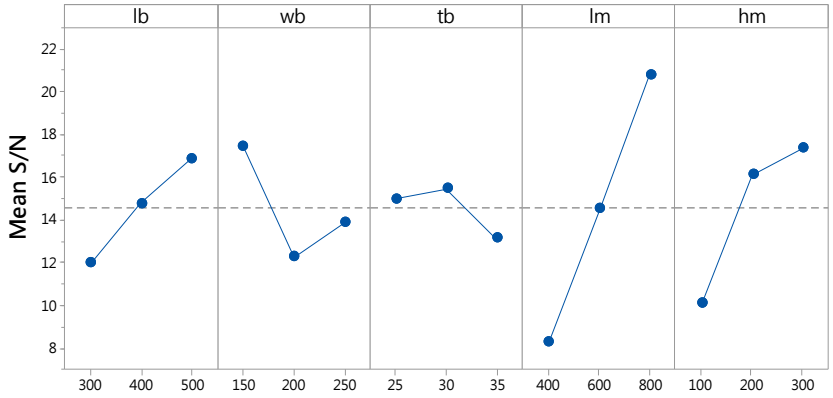

Fig. 5 Effect plot for the S/N of accelerometer gain

Table 5 FEM simulation data of the cross array design using a face-centered central composite design of 27 points and L16 to estimate S/N for the RSM using a quadratic model

L_{18}	l_b (μm)	w_b (μm)	t_b (μm)	l_m (μm)	h_m (μm)	Average Gain* $\beta_{average}$ (10^{-2} mV/G)	Standard Deviation* (10^{-2} mV/G)	S/N* (dB)
1	300	150	25	400	300	4.09	0.86	11.69
2	300	150	25	800	100	9.32	2.00	18.82
3	300	150	35	400	100	1.29	0.23	1.81
4	300	150	35	800	300	10.27	1.89	19.82
5	300	250	25	400	100	1.52	0.31	3.11
6	300	250	25	800	300	11.84	2.52	20.91
7	300	250	35	400	300	1.40	0.25	2.51
8	300	250	35	800	100	3.01	0.56	9.15
9	500	150	25	400	100	4.22	0.87	11.99
10	500	150	25	800	300	33.09	7.09	29.83
11	500	150	35	400	300	3.89	0.70	11.39
12	500	150	35	800	100	8.37	1.55	18.03
13	500	250	25	400	300	4.59	0.95	12.72
14	500	250	25	800	100	9.83	2.09	19.30
15	500	250	35	400	100	1.64	0.29	3.89
16	500	250	35	800	300	10.63	1.94	20.11
17	300	200	30	600	200	4.38	0.85	12.38
18	500	200	30	600	200	7.57	1.46	17.12
19	400	150	30	600	200	7.80	1.51	17.38
20	400	250	30	600	200	4.84	0.93	13.24
21	400	200	25	600	200	8.35	1.76	17.89
22	400	200	35	600	200	4.49	0.81	12.63
23	400	200	30	400	200	2.57	0.49	7.76
24	400	200	30	800	200	11.02	2.15	20.38
25	400	200	30	600	100	3.88	0.75	11.30
26	400	200	30	600	300	7.26	1.40	16.76
27	400	200	30	600	200	5.95	1.15	15.03

* Estimations using L16 outer array for the eight significant noise factors

3.4. Robust design of Micro-accelerometer using SURO

Instead of the cross array design in the Taguchi experimental design, this study integrates control and noise factors into a combined orthogonal array that serves as training samples for a surrogate model using ANN. All factors are selected as three-Level for the leaning samples, and two-level for the validation samples. The level settings of the validation samples are selected in between the levels of the learning samples as shown in Table 6. Total 11 factors including control factors of l_b, w_b, t_b, l_m, h_m and six noise factors of ω, t_p, E_p, E_{si}, ε_1, d_{31} are arranged in a combined orthogonal array of L27 as the learning samples and L16 as the validation samples. Although the operating frequency ω is not significant to the sensor gain from the ANOVA in section 3.2, this study still includes ω in the surrogate since the inclusion of the factor will not increase the size of training samples.

Table 6 Factors and levels for the experimental design of training samples.

	Learning samples			Validation samples	
	Level 1	Level 2	Level 3	Level 1	Level 2
Length of beam suspension l_b	300	400	500	350	450
Width of beam suspension w_b	150	200	250	175	225
Thickness of beam suspension t_b	25	30	35	27.5	32.5
Length of the seismic mass l_m	400	600	800	500	700
Thickness of the seismic mass h_m	100	200	300	150	250
Frequency ω	60	2500	5000	1250	3750
Thickness of PZT thin films t_p	0.9	1	1.1	0.95	1.05
PZT Young's Modulus E_{PZT}	71.42	79.36	87.3	75.54	83.33
Silicon<100> Young's Modulus E_{Si}	167.8	170	171.8	169.3	170.3
PZT Permittivity ε (10^{-9}F/m)	5.81	6.46	7.11	6.14	6.78
PZT Piezoelectric coefficient d_{31} (10^{-12} C/N)	-103.5	-93.5	-83.5	-98.5	-88.5

Table 7 L27 FEM simulation data of the learning samples of ANN

L_{27}	l_b (μm)	w_b (μm)	t_b (μm)	l_m (μm)	h_m (μm)	ω (Hz)	t_p (μm)	E_{PZT} (GPa)	E_{Si} (GPa)	ε (10^{-9} F/m)	d_{31} (10^{-12} C/N)	Gain (10^{-2} mV/G)
1	300	150	25	400	100	60	0.9	71.42	167.8	5.81	-10.35	2.565
2	300	150	25	400	200	2500	1.0	79.36	170.0	6.46	-9.35	3.329
3	300	150	25	400	300	5000	1.1	87.30	171.8	7.11	-8.35	3.985
4	300	200	30	600	100	60	0.9	79.36	170.0	6.46	-8.35	2.609
5	300	200	30	600	200	2500	1.0	87.30	171.8	7.11	-10.35	4.933
6	300	200	30	600	300	5000	1.1	71.42	167.8	5.81	-9.35	6.045
7	300	250	35	800	100	60	0.9	87.30	171.8	7.11	-9.35	3.224
8	300	250	35	800	200	2500	1.0	71.42	167.8	5.81	-8.35	4.784
9	300	250	35	800	300	5000	1.1	79.36	170.0	6.46	-10.35	7.767
10	400	150	30	800	100	2500	1.1	71.42	170.0	7.11	-10.35	10.390
11	400	150	30	800	200	5000	0.9	79.36	171.8	5.81	-9.35	15.198
12	400	150	30	800	300	60	1.0	87.30	167.8	6.46	-8.35	18.388
13	400	200	35	400	100	2500	1.1	79.36	171.8	5.81	-8.35	1.750
14	400	200	35	400	200	5000	0.9	87.30	167.8	6.46	-10.35	2.243
15	400	200	35	400	300	60	1.0	71.42	170.0	7.11	-9.35	2.010
16	400	250	25	600	100	2500	1.1	87.30	167.8	6.46	-9.35	5.941
17	400	250	25	600	200	5000	0.9	71.42	170.0	7.11	-8.35	4.549
18	400	250	25	600	300	60	1.0	79.36	171.8	5.81	-10.35	9.944
19	500	150	35	600	100	5000	1.0	71.42	171.8	6.46	-10.35	5.672
20	500	150	35	600	200	60	1.1	79.36	167.8	7.11	-9.35	7.898
21	500	150	35	600	300	2500	0.9	87.30	170.0	5.81	-8.35	9.036
22	500	200	25	800	100	5000	1.0	79.36	167.8	7.11	-8.35	11.230
23	500	200	25	800	200	60	1.1	87.30	170.0	5.81	-10.35	29.618
24	500	200	25	800	300	2500	0.9	71.42	171.8	6.46	-9.35	19.992
25	500	250	30	400	100	5000	1.0	87.30	170.0	5.81	-9.35	2.766
26	500	250	30	400	200	60	1.1	71.42	171.8	6.46	-8.35	2.499
27	500	250	30	400	300	2500	0.9	79.36	167.8	7.11	-10.35	3.113

The training samples consisted on L27 for learning samples as shown in Table 7 and L16 for validation samples are used to establish an artificial neural network using the toolbox of MATLAB. The input nodes of the ANN include the eleven factors as listed in Table 6. Two hidden layers are selected for the problem. A preliminary parameter study using Taguchi method was set up first to determine the optimal parameters for the training of ANN as follows: two hidden layers of 8 and 10 neurons with linear transfer function, Levenberg-Marquardt learning function, and the learning rate of 0.01. Adaptive learning network architecture is developed to train a back-propagation neural network as the surrogate model.

Real coded genetic algorithm is applied in this study to search in the subspace of the five control variables of the surrogate for the robust optimum with the following parameters:

1. Initialization:

(1) Number of population: 50
(2) Number of new offspring: 50
(3) Maximum generation: 100
(4) Parents selection method: roulette wheel selection

2. Crossover: single point crossover
3. Mutation: one point mutation with 0.3 mutation probability
4. Elitism: keep the best two organisms from the parent population to replace the worst two in the offspring.

The chromosome of every individuals considers only the control variables. A L16 soft outer array is selected to accommodate the eleven noise factors as in Table 1. For a given individual, the variations of the sensor gain β due to the noise factors can be estimated using the soft outer array to calculate the corresponding S/N from the recall of the ANN surrogate. The number of samples and the controlling costs of the outer array are then not a concern of the surrogate-based robust optimization since no actual experiment is conducted. Therefore, the operating frequency ω and the manufacturing tolerances of w_b and h_m that were excluded from the outer array in Taguchi method because of low significance are included in the soft outer array to better estimate of the stochastic distribution. The calculated S/N will become the fitness of individual in the evolution.

For the example of the initial design l_b= 400, w_b= 200, t_b= 30, l_m= 600, and h_m = 200 (μm), the soft outer array shown in Table 8 is applied to the design treatment to estimate the sensitivities of the 16 samples to calculate the S/N of the design. The S/N serves as the fitness in genetic algorithm. The searched optimum will be verified using the engineering system, which becomes the additional infilling sample to refine the ANN surrogate. The convergence of iterative NN-GA is reached if the last three searched optima are within 1/5000 of the diagonal Euclidean distance of the design space.

Fig. 6 shows a sample iteration result of SURO. The initial surrogate network started from 27 training samples and 16 validation samples, and the process converged after 15 iterations with a predicted S/N of 29.38 dB. Since only one verification of the nominal response of the predicted optimum is used as additional infilling sample in each iteration, the actual S/N of the robust optimum has to be evaluated using additional L16 engineering simulations. The verified S/N of the robust optimum is 29.85 dB which is very close to the average predicted value 29.53 dB of five runs from the ANN surrogate and the soft outer array. Although the predictions of the mean and standard deviation of the sensor gain from ANN are not as close to the verified results due to the surrogate from a relatively small set of training samples, the surrogate is good enough to provide an estimate of S/N to reach the robust optimum. The total number of experiments will add up to 74 in this optimization run. Table 9 shows the application of SURO to the sensor example in five runs, which all converge to the same robust optimum l_b= 500, w_b= 150, t_b= 25, l_m= 800, and h_m = 300 (μm) in average of 80.6 sample required.

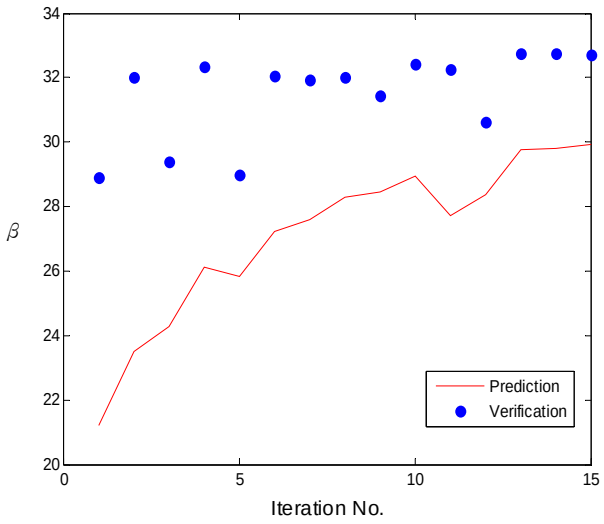

Fig. 6 Sample iteration of the iterative NN-GA

Table 8 Application of the ANN surrogate and the L16 soft outer array to estimate the S/N of a sensor design.

					ω	60	60	60	60	1700	1700	1700	1700	3350	3350	3350	3350	5000	5000	5000	5000			
					Δl_b	-2	-2	2	2	-2	-2	2	2	-2	-2	2	2	-2	-2	2	2			
					Δw_b	-2	-2	2	2	-2	-2	2	2	2	2	-2	-2	2	2	-2	-2			
					Δt_b	-2	-2	2	2	2	2	-2	-2	-2	-2	2	2	2	2	-2	-2			
					Δl_m	-2	-2	2	2	2	2	-2	-2	2	2	-2	-2	-2	-2	2	2			
					Δh_m	-2	2	-2	2	-2	2	-2	2	-2	2	-2	2	-2	2	-2	2			
					t_P	0.9	1.1	0.9	1.1	0.9	1.1	0.9	1.1	1.1	0.9	1.1	0.9	1.1	0.9	1.1	0.9			
					E_{PZT}	71.4	87.3	71.4	87.3	87.3	71.4	87.3	71.4	71.4	87.3	71.4	87.3	87.3	71.4	87.3	71.4			
					E_{Si}	167.8	171.8	167.8	171.8	171.8	167.8	171.8	167.8	171.8	167.8	171.8	167.8	167.8	171.8	167.8	171.8			
					ε	5.814	7.107	7.107	5.814	5.814	7.107	7.107	5.814	5.814	7.107	7.107	5.814	5.814	7.107	7.107	5.814			
					d_{31}	-103.5	-83.5	-83.5	-103.5	-103.5	-83.5	-83.5	-103.5	-83.5	-103.5	-103.5	-83.5	-83.5	-103.5	-103.5	-83.5			
l_b	w_b	t_b	l_m	h_m	No.	1	2	3	4	5	6	7	8	9	10	11	12	13	14	15	16	Mean Gain (10^{-2} mV/G)	Standard deviation (10^{-2} mV/G)	S/N (dB)
400	200	30	600	200	NN-predict	6.93	6.93	6.97	6.94	6.98	7.00	6.93	6.93	6.94	7.34	6.93	7.10	6.96	6.93	7.04	6.94	6.99	0.11	16.88

* Units of factors are as in Table 1

** The parameter values of t_p, E_{PZT}, E_{Si}, ε, and d_{31} are the tolerance ranges by applying the specification of tolerances in Table 1 to the thickness of PZT thin film and the typical material properties used in this study: t_p = 1 (μm), Silicon E_{Si} = 169.8 (GPa), PZT E_{PZT} = 79.36 (GPa), PZT Permittivity $\varepsilon = 6.4605\times10^{-9}$ (F/m), and PZT Piezoelectric coefficient $d_{31} = -93.5\times10^{-12}$ (C/N).

3.5. Comparison of Results

The comparison of the robust optimization results using Taguchi method, RSM, and SURO are presented in Table 9. The verified mean gain of the accelerometer provided by Taguchi method is 24.02×10^{-2} mV/G with a standard deviation of 5.55×10^{-2} mV/G. The verified mean gain of the design provided by SURO is 33.75×10^{-2} mV/G with a standard deviation of 8.24×10^{-2} mV/G. The design objective is to increase the sensor gain using the S/N_{STB} as a measure that considers both the mean and standard deviation of response. The robust optimum provided by SURO increases the S/N by 11% which stands for a reduction of the average quality loss by 48% compared with the one from Taguchi method, and reduced 73% of the number of experiments compared with those of Taguchi method. The robust optimization using single RMS derived the same robust optimum as SURO but required more than five times of the experiments of SURO.

Table 9 Comparison of the robust optimal designs and total number of experiments required using Taguchi method, RSM, and SURO for the design of micro-accelerometer

						Verified result using L16 engineering simulations			
	l_b	w_b	t_b	l_m	h_m	Mean Gain (10^{-2} mV/G)	Standard deviation (10^{-2} mV/G)	S/N (dB)	Total number of experiments
Initial	400	200	30	600	200	6.27	1.44	15.31	N/A
Taguchi	500	150	30	800	300	24.02	5.55	26.97	304
RSM	500	150	25	800	300	33.75	8.24	29.85	448
SURO	500	150	25	800	300	33.75	8.24	29.85	80.6*
	Optimization using SURO					Prediction from ANN surrogate			
1	500	150	25	800	300	30.44	3.17	29.53	80
2	500	150	25	800	300	31.30	3.13	29.78	93
3	500	150	25	800	300	29.89	3.07	29.38	74
4	500	150	25	800	300	30.67	3.26	29.59	80
5	500	150	25	800	300	29.85	3.10	29.36	76

***** Average number of total samples required in five optimization runs

4. Conclusions

This study presents an efficient robust optimization scheme for expensive engineering applications to reduce the experimental cost. Taguchi method applies cross array design where well controlled experiments are required for parameter using ANOM. However, accurate control of noise level at the designated level of outer array experiments may be infeasible. The proposed scheme SURO establishes a surrogate model using ANN from an integrated design of experiments for control and noise factors. The experimental design reduces not only the number but also the control cost of experiments. Since the exact parameter values in the experiments can be used to train ANN, a rough control of parameter value for even distribution of samples is sufficient. The estimation of S/N from the soft outer array and surrogate model also greatly reduce the experiment efforts. The application of the proposed scheme to the design of a piezoelectric micro-accelerometer shows that the robust optimum derived from the iterative GA search and training of surrogate model provides a superior sensor design than Taguchi method and a quadratic RSM using a much smaller set of samples. The proposed scheme can be readily applied to industrial applications of robust optimization where sampling cost is expensive and a rigorous control of factorial level setting of noise factors is difficult.

Several issues can be addressed in the future study. The proposed scheme suggests a smaller combined array consisted of control and noise variables to establish an ANN surrogate, and uses the predicted optimum as additional samples to iteratively update the model. The proposed scheme is efficient by search the subspace of control variables and adopts a soft outer array to estimate the robustness measure. However, if the system is highly nonlinear and the initial samples are not properly selected, the insufficient generality of the iterative surrogate may result in a search trapped to a local optimum. A better infilling sampling considering both exploitation and exploration sampling will help ensure the global optimality and sampling efficiency. Also, from the case study of accelerometer design, SURO adopts Taguchi's S/N to search for a robust design with higher S/N. However, the robust optimum increases both the mean and the standard deviation of the gain. An alternative selection of robustness measure such as a weighted sum of the mean and standard deviation can be considered to tradeoff performance and quality issues.

5. Acknowledgements

This research was partly supported by the Ministry of Science and Technology (MOST), Republic of China (TAIWAN) under contract MOST 104-2221-E-327-025.

6. References

Benardos, P.G. and Vosniakos, G.C. (2002) Prediction of surface roughness in CNC face milling using neural networks and Taguchi's design of experiments. Robotics and Computer-Integrated Manufacturing 18 (5–6):343-354. doi:http://dx.doi.org/10.1016/S0736-5845(02)00005-4

Bhattacharya, M. (2013) Evolutionary Approaches to Expensive Optimisation. (IJARAI) International Journal of Advanced Research in Artificial Intelligence, 2 (3):53-59. doi:www.ijarai.thesai.org

Bota, A., Gella, F.J., and Canalias, F. (2000) Optimization of adenosine deaminase assay by response surface methodology. Clinica Chimica Acta 290 (2):145-157. doi:http://dx.doi.org/10.1016/S0009-8981(99)00165-5

Chen, J., Wong, D.S.H., Jang, S.S. and Yang, S.L. (1998), Product and process development using artificial neural-network model and information analysis. AIChE Journal, 44: 876–887. doi:10.1002/aic.690440413

Dellino, G., Kleijnen, J. P., and Meloni, C. (2012) Robust optimization in simulation: Taguchi and Krige combined, INFORMS Journal on Computing 24(3): 471-484

Elsayed, K. and Lacor, C. (2014) Robust parameter design optimization using Kriging, RBF and RBFNN with gradient-based and evolutionary optimization techniques, Applied Mathematics and Computation 236: 325-344

Forrester, A.I.J. and Keane, A.J. (2009) Recent advances in surrogate-based optimization. Progress in Aerospace Sciences 45 (1-3):50-79.

Gamage, P., Jayamaha, N.P., Grigg, N.P., and Nanayakkara, N.K.B.M.P. (2014) Comparative analysis of Taguchi's crossed array approach vs combined array approach to robust parameter design: A study based on apparel industry, Industrial Engineering and Engineering Management (IEEM), 2014 IEEE International Conference on, 9-12 Dec. pp 749-753. doi:10.1109/IEEM.2014.7058738

Hou, J. and Zhang, J. (2017) Robust optimization of the efficient syngas fractions in entrained flow coal gasification using Taguchi method and response surface methodology, *International Journal of Hydrogen Energy,* 42(8): 4908-4921.

Irad, B.G. (2005) On the use of data compression measures to analyze robust designs. Reliability, IEEE Transactions on reliability 54 (3):381-388. doi:10.1109/TR.2005.853280

Jin, Y., Olhofer, M. and Sendhoff, B. (2002) "A framework for evolutionary optimization with approximate fitness functions," Evolutionary Computation, IEEE Transactions on, 6 (5): 481-494.

Köksoy, O. (2008) A nonlinear programming solution to robust multi-response quality problem, Appl. Math. Comput. 196 (2): 603-612, doi: http://dx.doi.org/10.1016/j.amc.2007.06.023

Lin, B.T. and Yang, C.Y. (2017) Applying the Taguchi method to determine the influences of a microridge punch design on the deep drawing, Int J Adv Manuf Technol, 88(5):2109–2119. doi:10.1007/s00170-016-8911-y

Lin, D.K.J. and Tu, W. (1995) Dual response surface optimization, Journal of Quality Technology 27: 34-39.

Maghsoodloo, S., Ozdemir, G., Jordan, V., and Huang, C.-H. (2004) Strengths and limitations of Taguchi's contributions to quality, manufacturing, and process engineering, Journal of Manufacturing systems 23(2): 73-126.

Mondal, S.C., Ray, P.K., Maiti, J., (2014) Modelling robustness for manufacturing processes: a critical review, International Journal of Production Research 52(2): 521-538

Moyo, S., Gashe, B.A., Collison, E.K., and Mpuchane, S. (2003) Optimising growth conditions for the pectinolytic activity of Kluyveromyces wickerhamii by using response surface methodology. International Journal of Food Microbiology 85 (1–2):87-100. doi:http://dx.doi.org/10.1016/S0168-1605(02)00503-2.

Ouyang, L., Ma, Y., Byun, J.-H., Wang J., Tu Y. (2016) An interval approach to robust design with parameter uncertainty, International Journal of Production Research, 54(11):3201-3215. DOI: 10.1080/00207543.2015.1078920

Parr, J. M., Keane, A. J., Forrester, A. I. J. and Holden, C. M. E. (2012) Infill sampling criteria for surrogate-based optimization with constraint handling, Engineering Optimization, 44 (10): 1147-1166.

Picheral, L., Hadj-Hamou, K., and Bigeon, J. (2014) Robust optimization based on the Propagation of Variance method for analytic design models, International Journal of Production Research, 52(24): 7324–7338, doi:http://dx.doi.org/10.1080/00207543.2014.926597

Sarve, A., Sonawane, S.S., and Varma, M.N. (2015) Ultrasound assisted biodiesel production from sesame (Sesamum indicum L.) oil using barium hydroxide as a heterogeneous catalyst: Comparative assessment of prediction abilities between response surface methodology (RSM) and artificial neural network (ANN). Ultrason Sonochem 26:218-228. doi:10.1016/j.ultsonch.2015.01.013

Seidel, H., Csepregi, L., Heuberger, and Baumgärtel, H. (1990) Anisotropic Etching of Crystalline Silicon in Alkaline Solutions. J Electrochemical Soc 137 (11):3626-3632

Su, C.T., Lin, C.M., and Chang, C. (2012) Optimization of the bistability property for flexible display by an integrated approach using Taguchi methods, neural networks and genetic algorithms. Microelectronics Reliability 52 (7):1492-1500. doi:http://dx.doi.org/10.1016/j.microrel.2012.02.025

Sun, G., Fang, J., Tian, X., Li, G., and Li, Q. (2015) Discrete robust optimization algorithm based on Taguchi method for structural crashworthiness design. Expert Systems with Applications 42 (9):4482-4492. doi:http://dx.doi.org/10.1016/j.eswa.2014.12.054

Sze, S.M. (1994) Semiconductor Sensors.

Taguchi, G. (1978) Performance analysis design. International Journal of Production Research 16 (6):521-530. doi:10.1080/00207547808930043

Tenne, Y. (2012) A computational intelligence algorithm for expensive engineering optimization problems. Engineering Applications of Artificial Intelligence 25 (5):1009-1021

Van Kampen, R.P. and Wolffenbuttel, R.F. (1998) Modeling the mechanical behavior of bulk-micromachined silicon accelerometers. Sensors and Actuators A: Physical 64 (2):137-150. doi:http://dx.doi.org/10.1016/S0924-4247(98)80007-1

Vining G. G. and Myers R. H., (1990) Combining Taguchi and response surface philosophies: a dual response approach, Journal of quality technology 22(1): 38-45

Xu, B., Cross, L.E., and Bernstein, J.J. (2000) Ferroelectric and antiferroelectric films for microelectromechanical systems applications. Thin Solid Films 377–378:712-718. doi:http://dx.doi.org/10.1016/S0040-6090(00)01322-5

Yang, B., Zhu, Y., Wang, X., Liu, J.Q., Chen, X., and Yang, C. (2014) High performance PZT thick films based on bonding technique for d31 mode harvester with integrated proof mass. Sensors and Actuators A: Physical 214:88-94. doi:http://dx.doi.org/10.1016/j.sna.2014.04.031

Yeniay, O., Unal, R., and Lepsch, R.A. (2006) Using dual response surfaces to reduce variability in launch vehicle design: A case study. Reliability Engineering & System Safety 91 (4):407-412. doi:http://dx.doi.org/10.1016/j.ress.2005.02.007

Yu, J.C. and Lan, C.B. (2001) System modeling of microaccelerometer using piezoelectric thin films. Sensors and Actuators A: Physical 88 (2):178-186. doi:http://dx.doi.org/10.1016/S0924-4247(00)00502-1

Yu, J.C. and Juang, J.Y. (2010) Design optimization of extrusion blow molded parts using prediction reliability guided search of evolving network modeling, Journal of applied polymer science, 117 (1): 222-234.

Zeidenberg, M. (1990) Neural Network Models in Artificial Intelligence (Ellis Horwood Series in Artificial Intelligence). Ellis Horwood Series in Artificial Intelligence.

Wang, G. J., Tsai, J. C., Tseng, P. C. and Chen, T. C. (1998) Neural-Taguchi Method for Robust Design Analysis, Journal of the Chinese Society of Mechanical Engineers 19 (2): 223-230.